PCCP

ROYAL SOCIETY OF CHEMISTRY

PAPER

View Article Online
View Journal

Cite this: DOI: 10.1039/d6cp00303f

Mechanistic insights into the stepwise oxidation of methane to methanol and formaldehyde over Cu-exchanged SSZ-13

Shotaro Okamoto,[a] Hajime Suzuki,[a] Tomoya Tashiro,[a] Junya Ohyama[b] and Keisuke Takahashi*[ac]

Received 28th January 2026,
Accepted 9th February 2026

DOI: 10.1039/d6cp00303f

rsc.li/pccp

The partial oxidation of methane to methanol is investigated over Cu-exchanged SSZ-13 using grid-based projector augmented wave within density functional theory and FDMNES XANES simulations. CH_4 activation at the Cu–O site proceeds, followed by CH_3OH oxidation to HCHO. Projected density of states analysis shows hybridization of the O 2p, Cu 3d, and H 1s orbitals at the transition states, confirming C–H bond activation at the Cu–O moiety. FDMNES simulations reveal a red shift in the Cu K-edge during both steps, indicating Cu reduction and its participation in the redox cycle. These results demonstrate that Cu–O sites are responsible for both methane activation and methanol oxidation with high selectivity toward partial oxidation products.

1. Introduction

Partial oxidation of methane to methanol is of great interest due to its potential to directly convert abundant natural gas into a valuable liquid fuel and chemical feedstock under mild conditions, offering a more efficient and sustainable alternative to conventional multi-step syngas-based processes.[1–5] Cu-exchanged zeolite is known as a promising catalyst for the selective oxidation of methane to methanol, owing to its isolated Cu sites that can be considered as activating methane at relatively low temperatures with high selectivity toward methanol formation.[6–8] However, the catalytic mechanism of Cu-exchanged zeolites remains unclear. Extensive studies have been conducted to unveil how Cu species are incorporated into the zeolite framework and to identify the nature of the active sites responsible for methane activation.[9–13]

In such circumstances, another question also arises, as the partial oxidation of methane over Cu-exchanged zeolites also produces formaldehyde.[13,14] It remains unclear whether formaldehyde is formed as a primary intermediate *en route* to methanol or as a byproduct through the overoxidation of methanol. The active sites responsible for formaldehyde formation over zeolites are not well understood. Here, SSZ-13 is investigated because Cu-exchanged SSZ-13 has been reported to be an active catalyst for methane oxidation.[15–19] Thus, density functional theory calculations are performed on Cu-exchanged SSZ-13 to identify the reaction mechanisms and identify the active sites involved in the selective formation of methanol and formaldehyde from methane.

2. Methods

Grid-based projector-augmented wave (GPAW) is implemented within density functional theory.[20] The exchange correlation of Perdew–Burke–Ernzerhof[21] along the spin polarization is implemented. Periodic boundary conditions are applied with the special K point of $(2 \times 2 \times 2)$ with a grid spacing of 0.18 Å.[22] A climbing-image nudged elastic band method by considering 6 images between each state is used for searching the transition state.[23] Finite difference method near edge structure (FDMNES) method is used for XANES simulation where the K-edge is used with a radius of 6 Å where the Green's function formalism is used for the electronic structure calculation, and the energy range is set from −5 eV to +30 eV relative to the Fermi energy.[24]

3. Results and discussion

Cu embdedded SSZ-13 zeolite is investigated through density functional theory. Atomic model is shown in Fig. 1 where the unit cell parameters in this work are 9.37 Å, 9.46 Å, and 9.44 Å. The atomic model is shown in Fig. 1. Two Si atoms are replaced with Al atoms to create Cu adsorption sites, and subsequently,

[a] Department of Chemistry, Hokkaido University, North 10, West 8, Sapporo 060-0810, Japan. E-mail: keisuke.takahashi@sci.hokudai.ac.jp
[b] Faculty of Advanced Science and Technology, Kumamoto University, Kumamoto 860-8555, Japan
[c] List Sustainable Digital Transformation Catalyst Collaboration Research Platform, Institute for Chemical Reaction Design and Discovery, Hokkaido University, Sapporo 001-0021, Japan

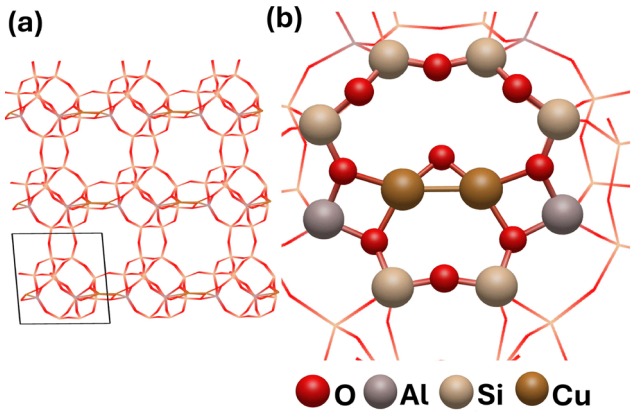

Fig. 1 Atomic model of the Cu-embedded SSZ-13 structure. (a) Periodic boundary conditions and (b) active site structure from (a).

two Cu atoms are placed at these Al sites. The stepwise conversion of CH_4 to CH_3OH and HCHO proceeds over Cu-embedded SSZ-13. The calculated energy diagram, including transition states and atomic structures, appears in Fig. 2(a) and (b). The first step involves hydrogen dissociation from CH_4, with the H atom binding to a nearby O atom and a transition state energy of 0.44 eV. The dissociated H then relocates to the side of the O atom, while CH_3 adsorbs onto the O atom, forming CH_3OH with a transition state energy of 0.12 eV; thus, CH_3OH is formed. One can see that the CH_3OH adsorption energy is calculated to be −2.26 eV, which is in good agreement with previous work.[25] In addition, these results agree with previous reports.[26]

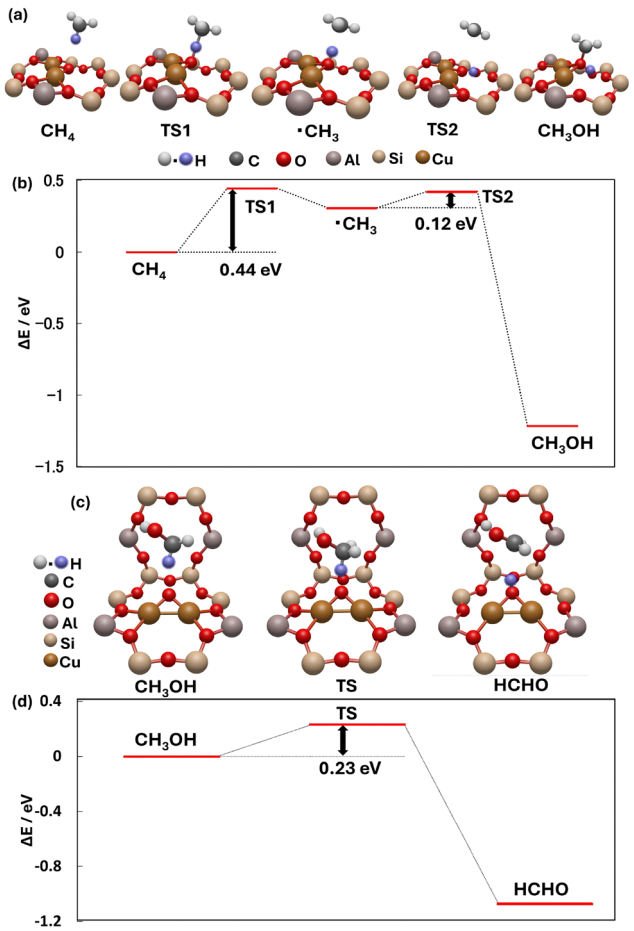

Fig. 2 Energy diagram with corresponding transition states and atomic structure for CH_4 to CH_3OH (a) and (b), and CH_3OH to HCCO (c) and (d).

Assuming that the produced CH_3OH desorbs from the Cu site, regeneration of an O atom on the same or a neighboring Cu site can provide the active site for further CH_3OH activation to HCHO. Therefore, the CH_3OH to HCHO reaction over the Cu active site is calculated. CH_3OH is placed on the Cu site as shown in Fig. 2(c) and (d). A transition state calculation is performed for H atom dissociation from CH_3OH, where the H atom is adsorbed on the O atom at the top of the Cu site. However, upon forming CH_2OH, the intermediate spontaneously rearranges to CH_2O with the H atom bound to a neighboring O atom during the relaxation process as shown in Fig. 2(c), indicating that CH_2OH is an unstable species. As a result, the calculated transition energy for CH_3OH to HCHO + H + H is 0.23 eV. Thus, the Cu site is considered to be an active site for CH_3OH to HCHO.

Electronic structure of the activation site is investigated *via* projected density of states (PDOS), as shown in Fig. 3. At TS1 in Fig. 2(a), the p state of the O atom overlaps with the H 1s orbital of CH_4, as well as with the d state of Cu, in an antibonding configuration. This interaction weakens the C–H bond, indicating that the O atom is responsible for activating CH_4, as shown in Fig. 3(b). At TS2 in Fig. 2(a), the s state of the H shifts to lower energy within the bonding region, indicating that the H atom is stabilized at the transition state. Lastly, TS in Fig. 2(c) demonstrates that the s state of H in CH_3OH, the p state of O and the d state of Cu are overlapping at antibonding state. Thus, electronic structures confirm that the Cu–O site is the active site for producing CH_4 and HCHO.

FDMNES simulations are performed to identify the electronic behavior of Cu during the reaction. The simulated XANES spectra for Cu in the CH_4 to CH_3OH and CH_3OH to HCHO conversion steps are presented in Fig. 4(a) and (b). Upon the formation of CH_3OH, the Cu absorption edge shifts toward lower energy, indicating a partial reduction of Cu during the CH_4 to CH_3OH conversion, as shown in Fig. 4(a). A similar red shift is observed in the CH_3OH to HCHO conversion, suggesting further reduction of the Cu center as shown in Fig. 4(b). This behavior indirectly indicates that Cu actively participates in the redox cycle, serving as the primary site for the activation and transformation of the C–H bond during both reaction steps.

Adsorption of the produced CH_3OH on Cu is calculated to be strongly exothermic, with an adsorption energy of −2.26 eV, as shown in Fig. 2(a). Such strong binding implies that desorption of CH_3OH from the Cu site must be carefully considered. Therefore, the CH_3OH desorption process is further investigated. Previous study suggests that co-adsorbed H_2O can facilitate the release of CH_3OH from Cu sites.[25] To examine this effect, an H_2O molecule is introduced to the CH_3OH adsorbed Cu site as shown in Fig. 5(a). Upon adsorption of H_2O, the CH_3OH adsorption energy becomes significantly weakened to −1.04 eV, while the H_2O adsorption energy is calculated to be −1.01 eV. In addition,

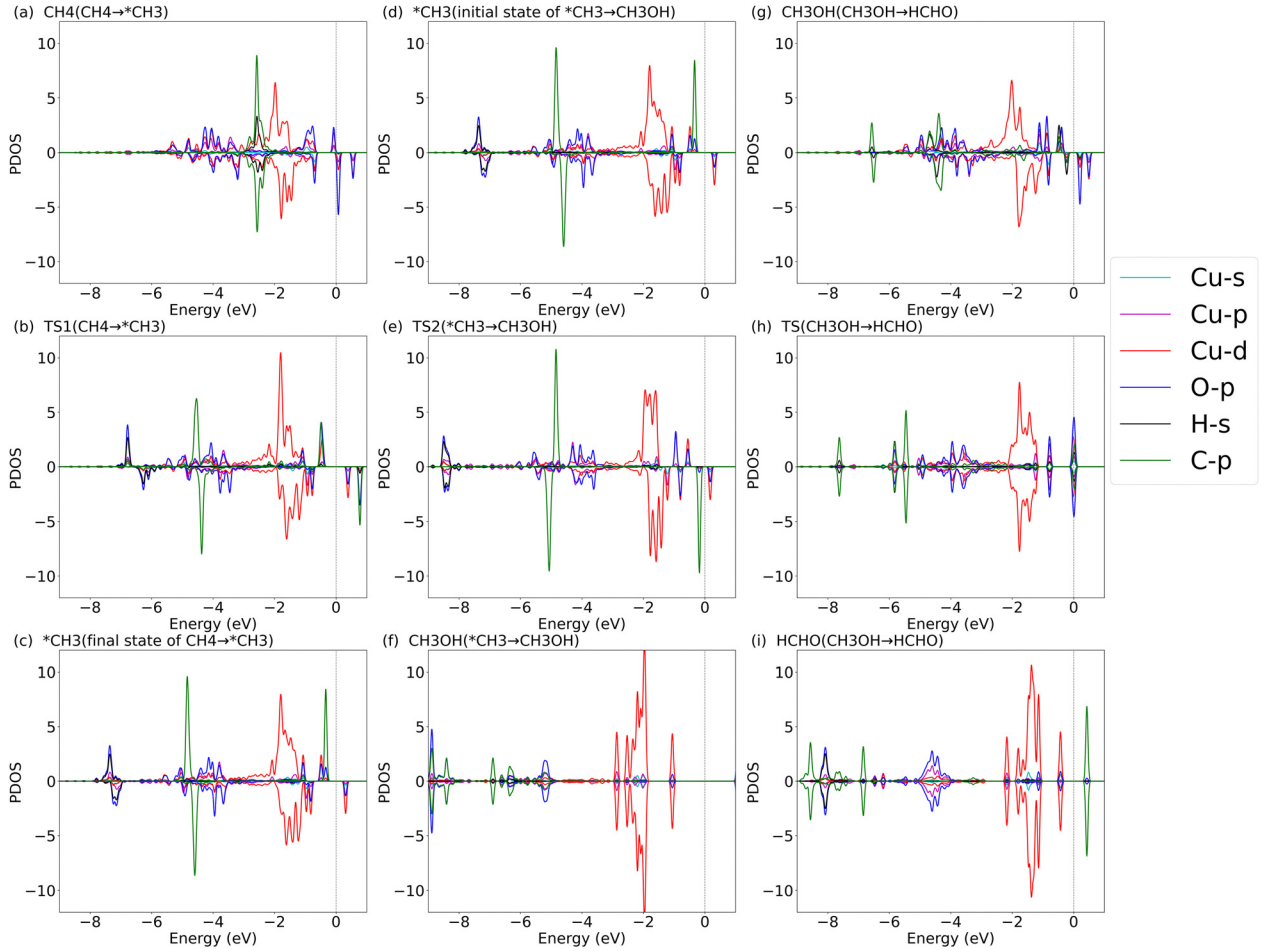

Fig. 3 Projected density of state at (a) CH_4, (b) TS1, (c) CH_3, (d) CH_3, (e) TS2, (f) CH_3OH, (g) CH_3OH, (h) TS, and (i) HCHO.

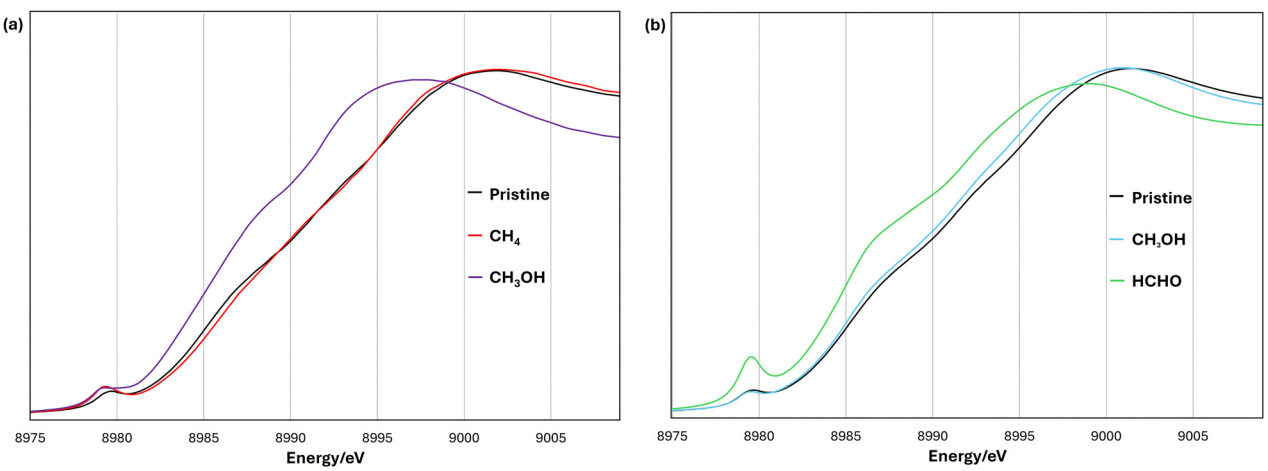

Fig. 4 FDMNES simulation for the Cu atom in (a) CH_4 to CH_3OH and (b) CH_3OH to HCHO.

the transition state energy barrier for CH_3OH desorption in the presence of H_2O is found to be 0.29 eV. Together, these results indicate that H_2O plays a crucial role in promoting CH_3OH desorption from Cu sites.

4. Conclusion

Density functional theory and FDMNES simulations are combined to elucidate the mechanism of methane partial oxidation over Cu-exchanged SSZ-13 zeolite. The DFT calculations reveal

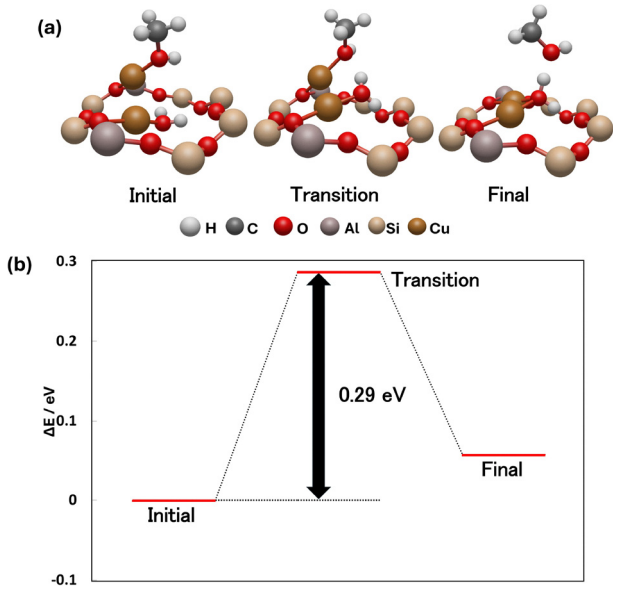

Fig. 5 Desorption of CH_3OH upon the adsorption of H_2O. (a) Atomic models and (b) the corresponding energy diagram.

that CH_4 is activated at the Cu–O site with an energy barrier of 0.44 eV, followed by CH_3OH formation and subsequent oxidation to HCHO with a barrier of 0.23 eV. The calculated energy diagram indicates that the transition states and adsorption energies fall within an energetically accessible range for the reaction. PDOS analysis demonstrates that the overlapping O 2p, Cu 3d, and H 1s orbitals at the transition states facilitate C–H bond cleavage. FDMNES simulations further indicate that the Cu K-edge shifts to lower energy during both reaction steps, evidencing a partial reduction of Cu and confirming its redox participation. Overall, these results establish that the Cu–O site functions as the active center for both CH_4 activation and CH_3OH oxidation, and that the redox dynamics of Cu are central to achieving selective methane oxidation in zeolitic catalysts.

Conflicts of interest

There are no conflicts to declare.

Data availability

Data will be made available upon request.

Acknowledgements

This work is funded by the Japan Science and Technology Agency (JST), ERATO grant number (JPMJER1903), JST Mirai Program Grant Number JP-MJMI25G1, and JSPS KAKENHI Grant-in-Aid for Scientific Research (B) Grant Number (JP23H01762) and (24K01241).

References

1 H. D. Gesser, N. R. Hunter and C. B. Prakash, The direct conversion of methane to methanol by controlled oxidation, *Chem. Rev.*, 1985, **85**, 235–244.
2 M. Brown and N. Parkyns, Progress in the partial oxidation of methane to methanol and formaldehyde, *Catal. Today*, 1991, **8**, 305–335.
3 M. Ravi, M. Ranocchiari and J. A. van Bokhoven, The direct catalytic oxidation of methane to methanol—a critical assessment, *Angew. Chem., Int. Ed.*, 2017, **56**, 16464–16483.
4 A. A. Latimer, A. Kakekhani, A. R. Kulkarni and J. K. Nørskov, Direct methane to methanol: the selectivity-conversion limit and design strategies, *ACS Catal.*, 2018, **8**, 6894–6907.
5 M. Ravi, V. L. Sushkevich, A. J. Knorpp, M. A. Newton, D. Palagin, A. B. Pinar, M. Ranocchiari and J. A. van Bokhoven, Misconceptions and challenges in methane-to-methanol over transition-metal-exchanged zeolites, *Nat. Catal.*, 2019, **2**, 485–494.
6 M. H. Mahyuddin, A. Staykov, Y. Shiota and K. Yoshizawa, Direct conversion of methane to methanol by metal-exchanged ZSM-5 zeolite (Metal = Fe, Co, Ni, Cu), *ACS Catal.*, 2016, **6**, 8321–8331.
7 P. Tomkins, M. Ranocchiari and J. A. van Bokhoven, Direct conversion of methane to methanol under mild conditions over Cu-zeolites and beyond, *Acc. Chem. Res.*, 2017, **50**, 418–425.
8 M. H. Mahyuddin, T. Tanaka, A. Staykov, Y. Shiota and K. Yoshizawa, Dioxygen activation on Cu-MOR zeolite: theoretical insights into the formation of Cu_2O and Cu_3O_3 active species, *Inorg. Chem.*, 2018, **57**, 10146–10152.
9 E. M. C. Alayon, M. Nachtegaal, A. Bodi and J. A. van Bokhoven, Reaction conditions of methane-to-methanol conversion affect the structure of active copper sites, *ACS Catal.*, 2014, **4**, 16–22.
10 M. B. Park, S. H. Ahn, A. Mansouri, M. Ranocchiari and J. A. van Bokhoven, Comparative study of diverse copper zeolites for the conversion of methane into methanol, *ChemCatChem*, 2017, **9**, 3705–3713.
11 M. H. Mahyuddin, Y. Shiota, A. Staykov and K. Yoshizawa, Theoretical overview of methane hydroxylation by copper-oxygen species in enzymatic and zeolitic catalysts, *Acc. Chem. Res.*, 2018, **51**, 2382–2390.
12 M. H. Mahyuddin, Y. Shiota and K. Yoshizawa, Methane selective oxidation to methanol by metal-exchanged zeolites: a review of active sites and their reactivity, *Catal. Sci. Technol.*, 2019, **9**, 1744–1768.
13 J. Ohyama, Y. Tsuchimura, A. Hirayama, H. Iwai, H. Yoshida, M. Machida, S. Nishimura, K. Kato and K. Takahashi, Relationships among the Catalytic Performance, Redox Activity, and Structure of Cu-CHA Catalysts for the Direct Oxidation of Methane to Methanol Investigated Using In Situ XAFS and UV-Vis Spectroscopies, *ACS Catal.*, 2022, **12**, 2454–2462.
14 N. V. Beznis, A. N. Van Laak, B. M. Weckhuysen and J. H. Bitter, Oxidation of methane to methanol and formaldehyde over Co-ZSM-5 molecular sieves: Tuning the

reactivity and selectivity by alkaline and acid treatments of the zeolite ZSM-5 agglomerates, *Microporous Mesoporous Mater.*, 2011, **138**, 176–183.

15 M. J. Wulfers, S. Teketel, B. Ipek and R. F. Lobo, Conversion of methane to methanol on copper-containing small-pore zeolites and zeotypes, *Chem. Commun.*, 2015, **51**, 4447–4450.

16 B. Ipek and R. F. Lobo, Catalytic conversion of methane to methanol on Cu-SSZ-13 using N_2O as oxidant, *Chem. Commun.*, 2016, **52**, 13401–13404.

17 K. Narsimhan, K. Iyoki, K. Dinh and Y. Román-Leshkov, Catalytic oxidation of methane into methanol over copper-exchanged zeolites with oxygen at low temperature, *ACS Cent. Sci.*, 2016, **2**, 424–429.

18 B. Ipek, M. J. Wulfers, H. Kim, F. Goltl, I. Hermans, J. P. Smith, K. S. Booksh, C. M. Brown and R. F. Lobo, Formation of $[Cu_2O_2]^{2+}$ and $[Cu_2O]^{2+}$ toward C–H bond activation in Cu-SSZ-13 and Cu-SSZ-39, *ACS Catal.*, 2017, **7**, 4291–4303.

19 R. Oord, J. E. Schmidt and B. M. Weckhuysen, Methane-to-methanol conversion over zeolite Cu-SSZ-13, and its comparison with the selective catalytic reduction of NO_x with NH_3, *Catal. Sci. Technol.*, 2018, **8**, 1028–1038.

20 J. Enkovaara, C. Rostgaard, J. J. Mortensen, J. Chen, M. Dułak, L. Ferrighi, J. Gavnholt, C. Glinsvad, V. Haikola and H. A. Hansen, *et al.*, Electronic structure calculations with GPAW: a real-space implementation of the projectoraugmented-wave method, *J. Phys.: Condens. Matter*, 2010, **22**, 253202.

21 J. P. Perdew, K. Burke and M. Ernzerhof, Generalized gradient approximation made simple, *Phys. Rev. Lett.*, 1996, **77**, 3865.

22 H. J. Monkhorst and J. D. Pack, Special points for Brillouin-zone integrations, *Phys. Rev. B: Solid State*, 1976, **13**, 5188.

23 G. Henkelman, B. P. Uberuaga and H. Jónsson, A climbing image nudged elastic band method for finding saddle points and minimum energy paths, *J. Chem. Phys.*, 2000, **113**, 9901–9904.

24 Y. Joly, O. Bunău, J.-E. Lorenzo, R.-M. Galera, S. Grenier and B. Thompson, Self-consistency, spin–orbit and other advances in the FDMNES code to simulate XANES and RXD experiments, *J. Phys.:Conf. Ser.*, 2009, 012007.

25 U. Engedahl, A. Boje, H. Strom, H. Gronbeck and A. Hellman, Complete reaction cycle for methane-to-methanol conversion over Cu-SSZ-13: first-principles calculations and microkinetic modeling, *J. Phys. Chem. C*, 2021, **125**, 14681–14688.

26 M. H. Mahyuddin, A. Staykov, Y. Shiota, M. Miyanishi and K. Yoshizawa, Roles of zeolite confinement and Cu–O–Cu angle on the direct conversion of methane to methanol by $[Cu_2(\mu\text{-}O)]^{2+}$-exchanged AEI, CHA, AFX, and MFI zeolites, *ACS Catal.*, 2017, **7**, 3741–3751.